Journal of Radioanalytical and Nuclear Chemistry
https://doi.org/10.1007/s10967-021-08070-7

Application of kaolinite-based composite as an adsorbent for removal of uranyl ions from aqueous solution: kinetics and equilibrium study

Zeynep Mine Şenol[1] · Zehra Seba Keskin[2] · Ali Özer[3] · Selçuk Şimşek[4]

Received: 19 August 2021 / Accepted: 18 October 2021

Abstract
Polyacrylamide (PAA)-kaolinite (K) composite adsorbent was synthesized using K and PAA hydrogel, in-situ polymerization method as synthesis method. Adsorbent performance of the PAA-K composite for UO_2^{2+} ions was optimized: 400 mg L^{-1} at pH 4.5 at 25 °C. Synthesized PAA-K composite was featured by FT-IR, SEM–EDX, and XRD techniques. The maximum UO_2^{2+} ions adsorption capacity of the PAA-K composite was found to be 0.0656 mol kg^{-1}. Thermodynamic parameters demonstrated that the behaviour of the adsorption was an endothermic and spontaneous. Finally, adsorption process suggested that the PAA-K composite had a significant adsorption capacity for the UO_2^{2+} ions.

Keywords Kaolinite · Polyacrylamide · Composite · Uranyl removal · Wastewater treatment

Introduction

Heavy metals found naturally in the earth's crust are important pollutants in water and wastewater due to their non-biodegradable and non-destructible structure [1]. Determination of heavy metals discharged from industrial activities into water bodies above the acceptable limit threatens public health and the ecosystem [2]. Uranium, heavy metal with chemical toxicity and radioactivity, exists in various forms under different conditions. The hexavalent uranyl ion (UO_2^{2+}), which is the most stable among these forms, causes irreversible kidney damage and increased carcinogenicity [3]. Also, uranium recovery is of great importance for the sustainable development of the nuclear industry. Therefore, it has become a very important issue to develop an effective method for removing and recovering uranium from water and wastewater.

✉ Zeynep Mine Şenol
msenol@cumhuriyet.edu.tr

[1] Department of Food Technology, Zara Vocational School, Cumhuriyet University, 58140 Sivas, Turkey

[2] Department of Food Technology, Cumhuriyet University, Yıldızeli Vocational School, 58140 Sivas, Turkey

[3] Department of Metallurgical and Materials Engineering, Cumhuriyet University, 58140 Sivas, Turkey

[4] Department of Chemistry, Sivas Cumhuriyet University, 58140 Sivas, Turkey

Recently, various methods have been used for the removal of uranyl ions from aqueous solutions such as membrane separation method [4], chemical precipitation [5], solvent extraction [6], ion Exchange[7], and adsorption [8–10] However, these methods have disadvantages such as high cost, secondary pollution, and ineffectiveness at low metal concentrations. Among these methods, adsorption, which is the most effective and convenient method for removing trace levels of ions, is of interest. Adsorption method has significant advantages for the treatment of heavy metal containing wastewater because of its advantages such as low cost, ease of application, high selectivity, environmental friendlines and high efficiency. The selection of the effective adsorbent is very significant in adsorption process. Because, an effective adsorbent should be an recyclable, economical, non-toxic, and easily accessible material. Many adsorbents have been used to remove heavy metal ions from aquatic solutions, such as chitosan [11], zeolite [12], bentonite [13], montmorillonite [14], dolomite [15], biomass [16], metal organic-frameworks [17].

Kaolinite is one of the well-known low-cost natural clays found in rocks as a crystalline structure. Kaoliniteite ($Al_2Si_2O_3(OH)_4$), the most important mineral of kaolinite, is a 1:1 aluminosilicate, whose layers are composed of a tetrahedral silica layer (SiO_4) bonded to an octahedral alumina layer (AlO_6) with shared oxygen atoms. The layers are held together by hydrogen bonding of adjacent silica and alumina layers [18]. Composed of metal oxides such as Al_2O_3, SiO_2,

Published online: 29 October 2021

MgO and CaO, kaolinite clay has become an indispensable material for many industrial processes due to its excellent performance such as good bonding ability, high whiteness, thermal stability and excellent electrical insulating property [19]. However, coagulation and aggregation, which is one of the negativities affecting the hydrodynamic properties of clays, limit its use. Some modification processes are carried out to improve and change these weaknesses of clays and increase their adsorption capacity. On the other hand, these problems can be eliminated by synthesizing a composite of kaolinite.

In this research, a novel composite was formed by using polyacrylamide hydrogel which is known as inert and has a high water holding capacity. Thus, the adsorption of UO_2^{2+} ions in the aqueous phase using this composite as the adsorbent was aimed. Synthesized PAA-K composite was characterized by FT-IR, SEM–EDX, XRD techniques. The aim of the research was to develop an effective adsorbent to be efficiently used for the elimination of contaminating industrial heavy metals in wastewaters. Thus many of the physical and chemical parameters of the adsorption were assessed.

Experimental

Chemicals

Acrylamide monomer (AA), N,N'-methylenebisacrylamide (MBSA), N,N,N',N'- tetramethylethylenediamine (TEMED) Sigma-Aldrich), Ammonium persulfate (APS), 4-(2-pyridylazo) resorcinol (PAR), $UO_2(NO_3)_2{\cdot}6H_2O$ (Merk) were used. Kaolinite mineral was obtained from Ankara Akmin Mining.

Characterization

For characterization of the synthesized PAA-K composite adsorbent were used Fourier Transform Infrared Spectroscopy (FT-IR, Perkin Elmer 400), scanning electron microscopy and Energy Dispersive X-ray Spectroscopy (TESCAN MIRA3 XMU) and X-ray diffraction (XRD, Bruker Axs D8 Advance Model). UO_2^{2+} ion concentration was determined by using a UV–vis spectrophotometer (SHIMADZU, 160 A model, Japan).

Preparation of PAA-K

PAA-K composite was synthesized using kaolinite and polyacrylamide, in-situ polymerization method as synthesis method. To this end, 10 mL of the solution including 2 g of AA monomer and 0.2 g of MBSA were added to 20 mL of the aquatic solution including 1 g of kaolinite, then vigorously stirred for 30 min. Then 400 mg of APS and 200 µL of TEMED were added to the polymerization reaction, respectively. PAA-Do composite was obtained and the obtained composite was washed with distilled water and then dried.

Adsorption procedure

To explore the optimal batch experimental conditions of UO_2^{2+} adsorption on PAA-K were studied the effects of pH, initial UO_2^{2+} concentration, adsorbent mass, contact time, temperature and desorption. This experiments were carried out the certain concentration of UO_2^{2+} (400 mg L^{-1}) and containing PAA-K (100 mg) in 10 mL the polypropylene tubes. The equilibrium concentration of UO_2^{2+} was determined by the absorbance measurement and by using the PAR method [20]. In this method, the concentration of UO_2^{2+} ions is formed spectrophotometrically as a selective complex with PAR at $\lambda = 530$ nm. Adsorption%, Q (mol kg^{-1}) and % Desorption were calculated with Eq. (1) and Eq. (2).

$$\text{Adsorption } \% = \left[\frac{C_i - C_f}{C_i}\right] \times 100\% \quad (1)$$

$$Q = \left[\frac{C_i - C_f}{m}\right] \times V \quad (2)$$

$$\text{Desorption } \% = \frac{Q_{des}}{Q_{ads}} \times 100\% \quad (3)$$

C_f is equilibrium UO_2^{2+} concentration (mg L^{-1}), C_i is the initial UO_2^{2+} concentration (mg L^{-1}), m refers to the adsorbent mass (g), V is the solution volume (L), Q_{des}; desorbed amount of UO_2^{2+} (mol kg^{-1}) and Q_{ads}; the adsorbed amount of UO_2^{2+} (mol kg^{-1}).

Results and discussion

FT-IR, SEM–EDX and XRD analysis

FT-IR analysis is a kind of vibrational spectroscopy and the FT-IR spectrums reflect the changes of functional groups on the surface of K, PAA and PAA-K composite. The changes on the peaks indicated the functional groups (Fig. 1). The peaks observed at 1035, 914, 797, 778 and 690 cm^{-1} corresponding to the kaolinite characteristic peaks. When the spectrum of kaolinite is examined, the peaks observed at 1035 cm^{-1} and 914 cm^{-1} correspond to Si–O stretching vibrations and Si–OH vibrations, respectively [21]. The peak determined at 792 cm^{-1} is due to Si–O-Al stretching

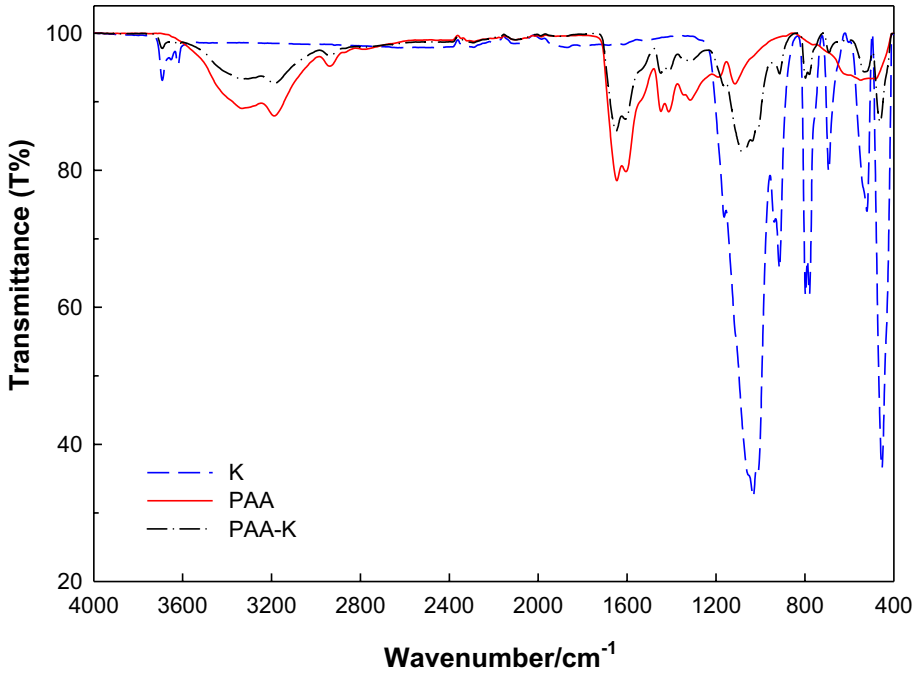

Fig. 1 FT-IR spectrums of K, PAA and PAA-K composite

vibrations, the peak at 769 cm^{-1} is due to Si–O-Al bending vibrations, and the peak at 690 cm^{-1} is due to Si–O-Si bending vibrations [22, 23]. In the FT-IR spectrum of PAA, the peak at 3190 cm^{-1} is attributed to the symmetrical vibrations of the amide group, the -CN stretching vibration of the amide group at 1425, the peaks observed at 2940 cm^{-1} and 1450 cm^{-1} are attributed to the stretching and bending vibrations of the CH_2 group, and the peak at 1650 cm^{-1} is attributed to the C = O (carbonyl group) stretch [24]. FT-IR spectrum of PAA-K composite is examined, it is seen that it is different from both spectra. The spectrum of the PAA-K composite is observed as the characteristic peaks of both PAA and kaolinite. In the PAA-K spectrum is observed peaks representing the C = O stretching vibration of the amide group at 1672 cm^{-1}, the $–NH_2$ bending vibration of the amide group at 3192 cm^{-1}, the -CN stretching vibration of the amide group at 1430 cm^{-1} in structures of the PAA. In the PAA-K spectrum is observed peaks representing Si–O stretching vibrations and Si–OH vibrations at 1073 and 916 cm^{-1}, the Si–O-Al stretching vibrations at 776 cm^{-1}, the Si–O-Si bending vibrations at 1430 cm^{-1} in structures of the kaolinite. These results showed that the PAA-K composite was successfully synthesized.

As in Fig. 2 for PAA, the organic sample has an irregular shape as a powder with a wide distribution of particles with an average of 200 microns. The organic surface is brittle fractured morphology. The kaoliniteite is an inorganic aluminasilicate mineral powder with a hydroxide structure. The dimensional stability of composites of PAA-K is similar to PAA with a smooth surface and kaoliniteite with rough powders. The composite particles are also about 200 microns while many average size particles were formed about 20 microns are still present. The red arrows show the high magnification images of as directed places. U species adsorbed on PAA-K composites may occur as precipitates and within polymer structure as seen in whiter regions on and in organic structures.

EDX analysis in Fig. 3 shows C and O as an organic structure, Al and Si along with O stand for kaoliniteite with a possible formula of $Al_2O_3.6SiO_2.nH_2O$ as seen from the spectrum as well. U species are seen as adsorbed within an organic matter with kaoliniteite doped composite. U as seen from the map image is deposited especially around the interlayers of kaoliniteite as well as the organic matter of composite material.

Figure 4 shows the XRD pattern of PAA, PAA-K before and after U doping. PAA has a hump-like organic structure pattern while having very tiny crystallization peaks at 33° 2thetas due to limited high volumetric orientation of C-H-N–O. After doping with U, a variety of U–O peaks are formed by the adsorption of U on PAA-K. The peaks at 20.3°, 24.7° and 33.2° 2thetas belong to U_3O_8 with a JCPDS file of 23–1460. U formula is a valance compound of U_2O_5 and UO_3 which is + 5 and + 6 U compound, respectively. At 24.9°, 26.1°, the peaks with tiny 29° and split peak at 35.9° and 36.2° belong to UO_3. All U related phases are shown with a diamond symbol to separate from other phases. Uraninite should have been considered as another phase having a main peak at 28.8° which has very low intensity on the pattern, 33.5° as a split peak. Increased oxygen also favors the formation of U_3O_8 that may be due to the existence of

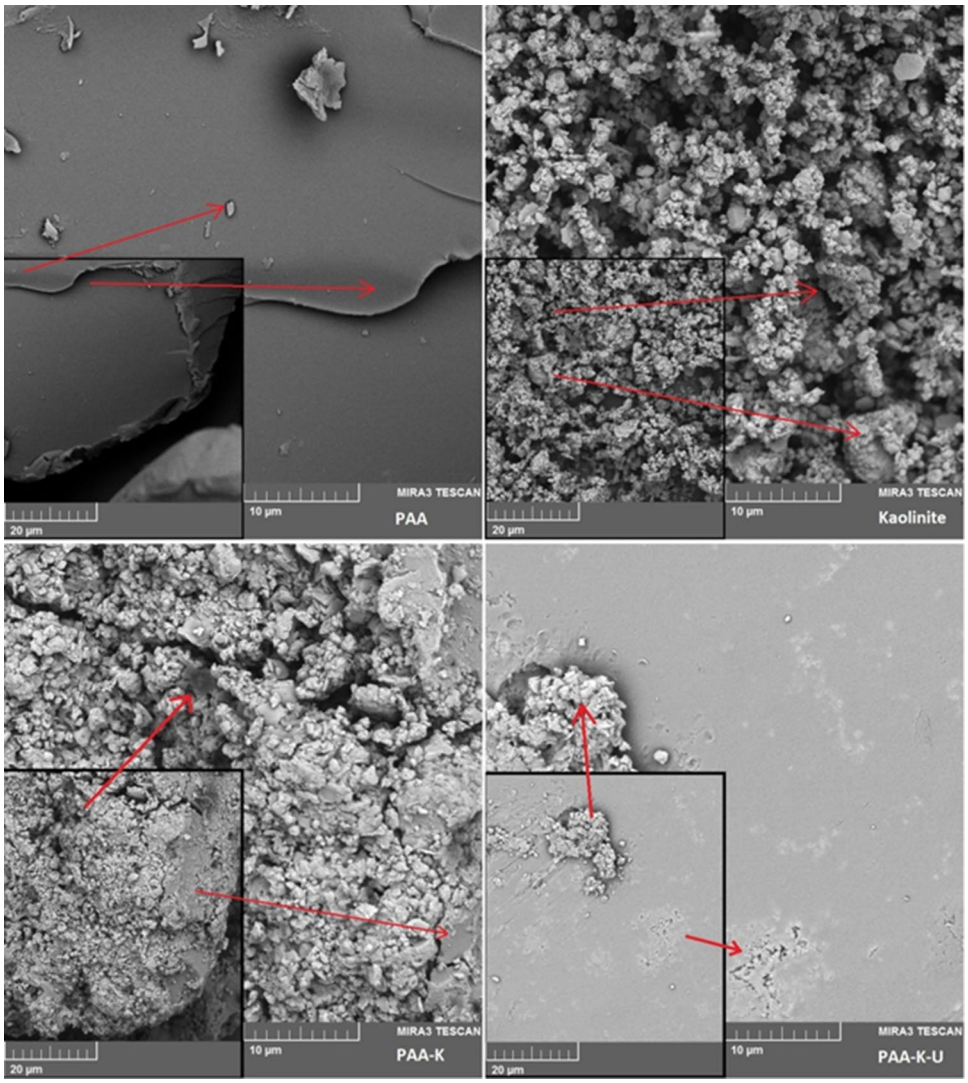

Fig. 2 SEM images of PAA, Kaolinite, PAA-K composite and U doped PAA-K composite and their corresponding inset lower magnification pictures

kaoliniteite and may also be exchanging of O ions with organic structure in the composite.

The distribution of phase-related peaks doesn't have main peaks initially, which could be concluded as fine nanosized (< 10 nm) oxide production may not be oriented to the main direction of common. The nano grains' orientation could be other than the main peak due to precipitation from the solution. Since the concentration of U is low even on the surface to obtain good intensities of main U–O related oxides only remains on the surface of the PAA-K composite.

Point of zero charge (PZC) for PAA-K and Effect of pH

The aqueous medium pH is one of the important factors in adsorption studies. Solution pH determines both the type of molecule or ion adsorbed in the solution and also changes the charge of the adsorbent surface. For this purpose, PZC study was conducted to find out how the adsorbent surface changes with ambient pH. The results are given in Fig. 5. The surface charge of the PAA-K composite adsorbent was found to be 2.87. This result showed that at pH below 2.87, the surface was predominantly positively charged. This is due to the high concentration of protons in the environment, the elimination of surface hydroxyl groups and the protonation of the surface.

At high pH, the presence of hydroxyl groups on the surface and the low number of H^+ ions in the solution caused the surface to be negative due to the increase in the number of negative charges on the surface is also given. It is quite less at low pH and with increasing pH, an increase in adsorption is observed. This result can be explained for two reasons. (I) The surface charge increases with increasing pH and the electrostatic interaction with the uranyl ion, which is the cationic species, increases, which causes an increase in adsorption. Considering the surface load, the PZC study supports the pH study. (II) A decrease in adsorption was observed due to competitive adsorption between

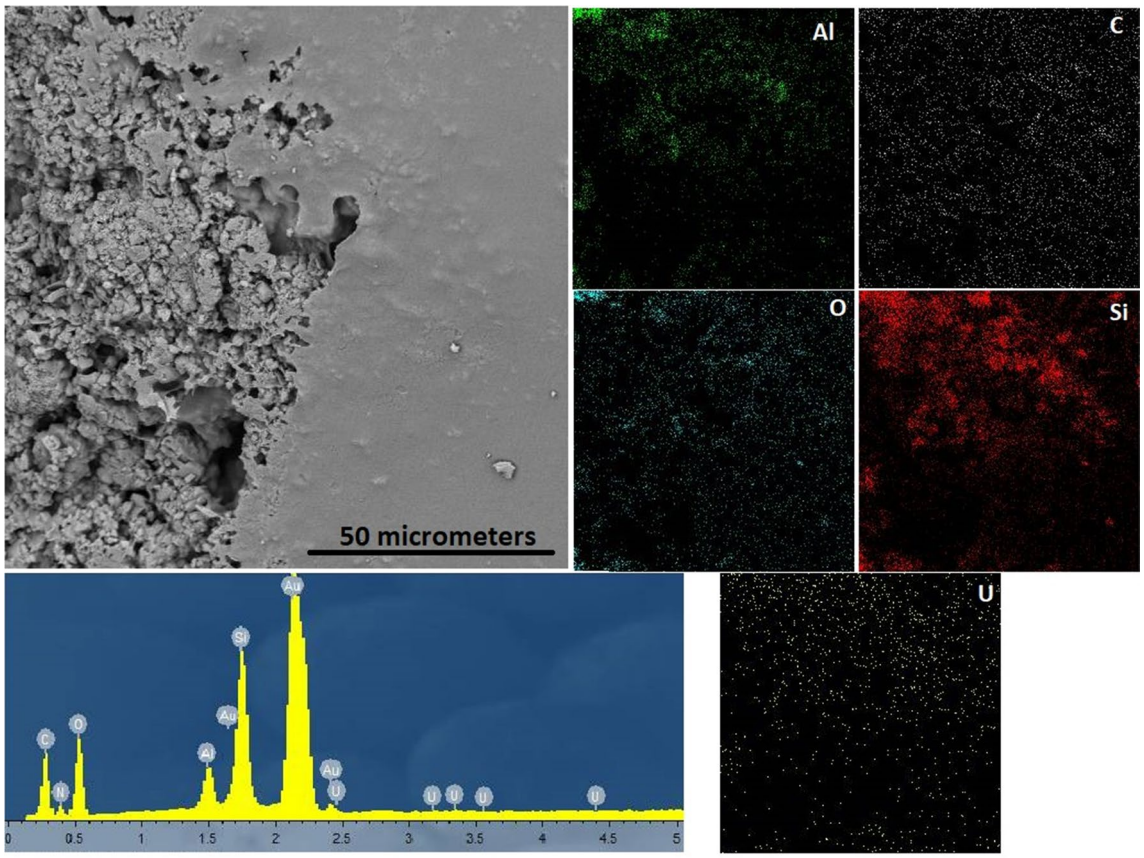

Elements	C	N	O	Al	Si	U	Total
wt%	33.82	9.19	30.79	4.34	20.13	1.73	100.00

Fig. 3 EDX map analysis of images as seen in the upper left and corresponding maps of related elements, spectrum on the lower left and weight distribution % of elements of PAA-K-U image

hydronium ions and uranyl ions at low pH. In addition, different polikatoynic species of uranyl at varying pH levels are effective in adsorption. At different pH the UO_2^{2+} ion was as hydrolysis form of UO_2^{2+} ion appearance, such as $UO_2(OH)^+$, and $(UO_2)_3(OH)_5^+$, while the hydrolysis form of UO_2^{2+} ion will affect the interaction between adsorbent and metal ions. The pHs > 5 values, precipitation of UO_2^{2+} ions such as $UO_2(OH)^+$, $UO_2(OH)_2^{2+}$ and $[(UO_2)_3(OH)_5]^+$ occurs. In this case may lead to misinterpretation of UO_2^{2+} adsorption [25]. Therefore, the pHs > 5 values have not been studied. The natural pH of UO_2^{2+} ions at 400 mg L^{-1} is 4.5.

Effect of adsorbent mass

The effect of the amount of PAA-K composite on the adsorption behavior of UO_2^{2+} ions was studied in the range of 10–200 g L^{-1} under the conditions of C_0: 400 mg L^{-1}, pH: 4.5, t: 1440 min, and T: 25 °C. The results obtained are presented in Fig. 6. It can be seen from Fig. 6, that the adsorption of UO_2^{2+} ions increased with the increase in the amount of PAA-K composite. The active centers on the surface of the PAA-K composite increase as the amount of adsorbent increases. Maximum adsorption was found to be approximately 70% in the amount of 20 g L^{-1} of PAA-K composite. The number of active binding centers has increased due to the increase in the amount of PAA-K composite. The increase in the adsorption efficiency of UO_2^{2+} ions is due to the increase of active binding centers for adsorption.

Adsorption isotherm models

Adsorption isotherms are curves created at different concentrations at constant temperature for the design of the adsorption process, understanding the adsorption mechanism and determining the adsorption capacity and surface properties of the adsorbent. By applying various adsorption models to

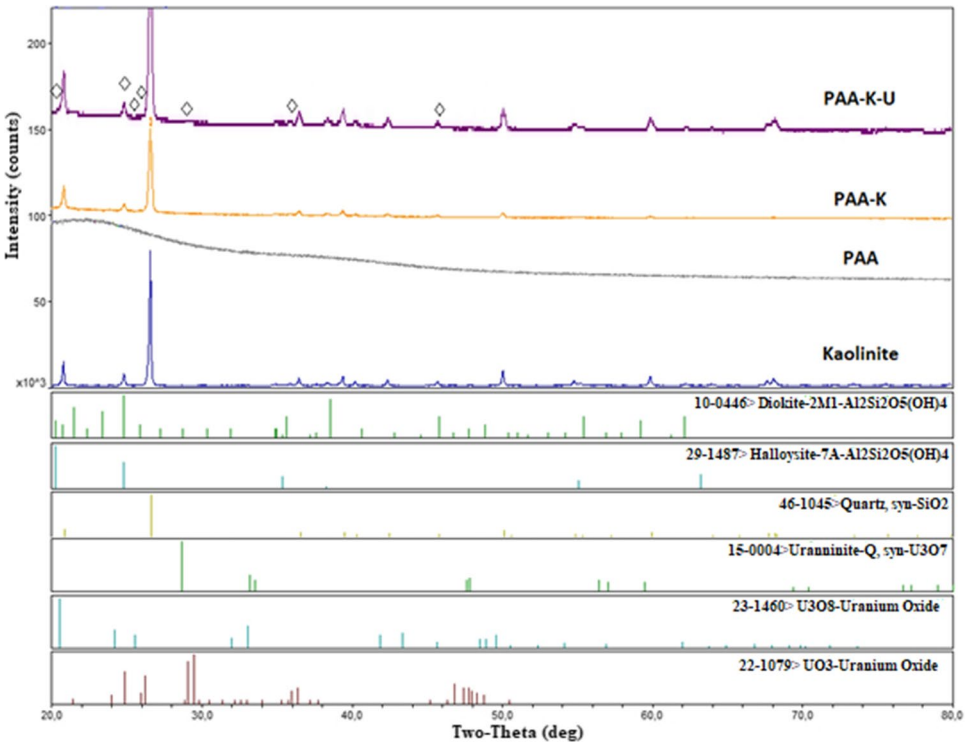

Fig. 4 XRD pattern of kaolinite, PAA, PAA-K and PAA-K-U composites and their corresponding JCPDS files

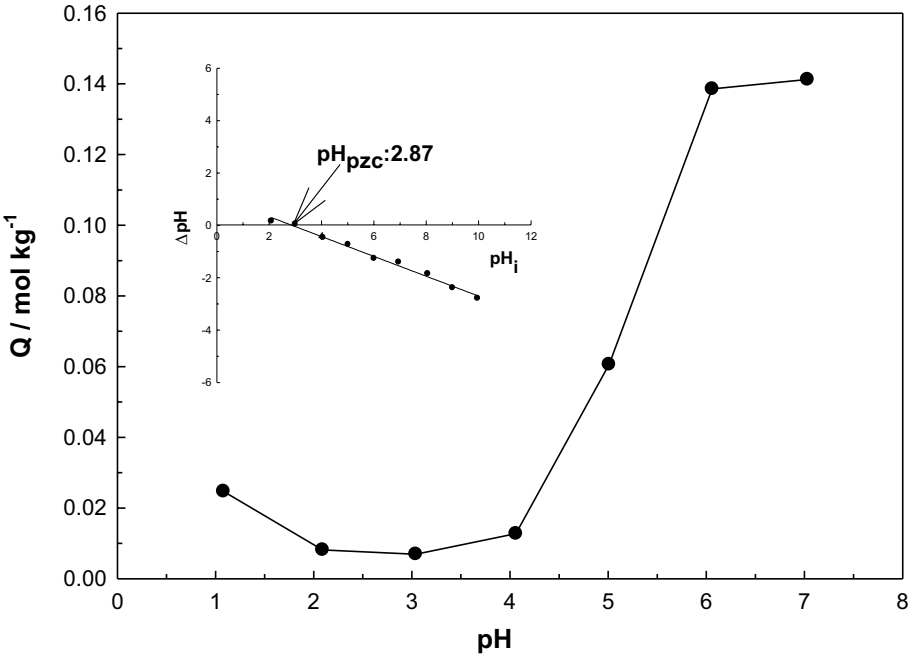

Fig. 5 Effect of pH on adsorption of UO_2^{2+} onto PAA-K {$[UO_2^{2+}]_0$:400 mg L^{-1}, adsorbent dosage: 100 mg, natural pH:1.0–7.0, contact time:24 h, temperature: 25 °C} and PZC for PAA-K

experimental data, parameters such as adsorption capacity, surface heterogeneity, and adsorption energy of adsorption are provided. Among the adsorption agents, the widely used modeler Langmuir, Freundlich and Dubinin-Radushkevich (D-R) are the isotherm models. Equations of these models are presented in Table 1.

At pH: 4.5, m: 100 mg, t: 1440 min, and T: 25 °C., the effects of different initial UO_2^{2+} ions concentrations (50–1000 mg L^{-1}) on the adsorption process of PAA-K composite were investigated. Compliance with the adsorption isotherm models for the adsorption of UO_2^{2+} ions to the PAA-K composite is presented in Fig. 7 and the derived isotherm parameters in Table 1. When Fig. 7 is

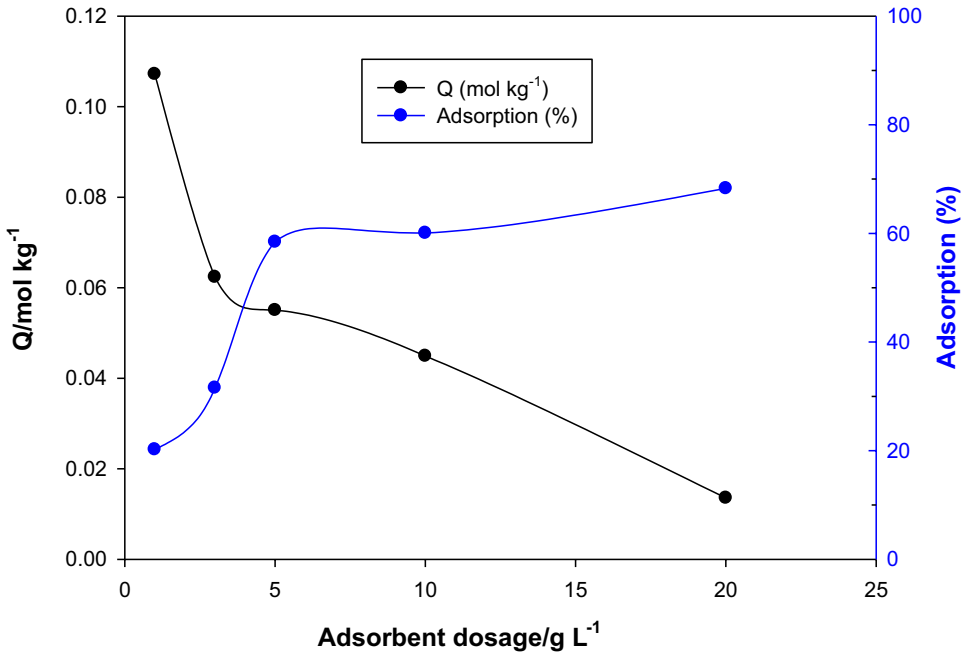

Fig. 6 Effect of adsorbent dosage on adsorption of UO_2^{2+} onto PAA-K {$[UO_2^{2+}]_0$:400 mg L^{-1}, adsorbent dosage:10, 30,50, 100 and 200 mg, natural pH:4.5, contact time:24 h, temperature: 25 °C}

Table 1 Langmuir, Freundlich and D-R isotherm models and their parameters

Isotherm models	Equation	Parameter
Langmuir	$Q = \frac{X_L K_L C_e}{1+K_L C_e}$	X_L: the maximum adsorption capacity K_L: the parameter for Langmuir isotherm Q: the amount of adsorbed UO_2^{2+} C_e: the equilibrium concentration
Parameter	Value	R^2
X_L (mol kg^{-1})	0.0656	0.948
K_L (L mol^{-1})	184	
Freundlich	$Q = K_F C_e^{\beta}$	K_F: Freundlich constant β: adsorbent surface heterogeneity
Parameter	Value	R^2
X_F	1.76	0.873
β	0.514	
D-R	$Q = X_{DR} e^{-K_{DR}\varepsilon^2}$ $\varepsilon = RTln(1+\frac{1}{C_e})$ $E_{DR} = (2K_{DR})$	X_{DR}: a measure of adsorption capacity K_{DR}: the activity coefficient ε: the Polanyi potential R: the ideal gas constant (8.314 $Jmol^{-1}$ K^{-1}) E_{DR}: the adsorption energy T: the absolute temperature
Parameter	Value	R^2
X_{DR} (mol kg^{-1})	0.238	0.898
$-K_{DR}x10^9/mol^2KJ^{-2}$	5.31	
E_{DR}/kJ mol^{-1}	9.71	

examined, the UO_2^{2+} ion adsorption efficiency was found to be high at low concentrations due to the empty active centers on the surface of the PAA-K composite adsorbent. At high concentrations, UO_2^{2+} ions adsorption decreased and stabilized due to the filling of all active centers on the PAA-K composite adsorbent surface.

When the R^2 values calculated from the Langmuir and Freundlich isotherm models were compared, it was seen that the adsorption process fit the Langmuir isotherm model

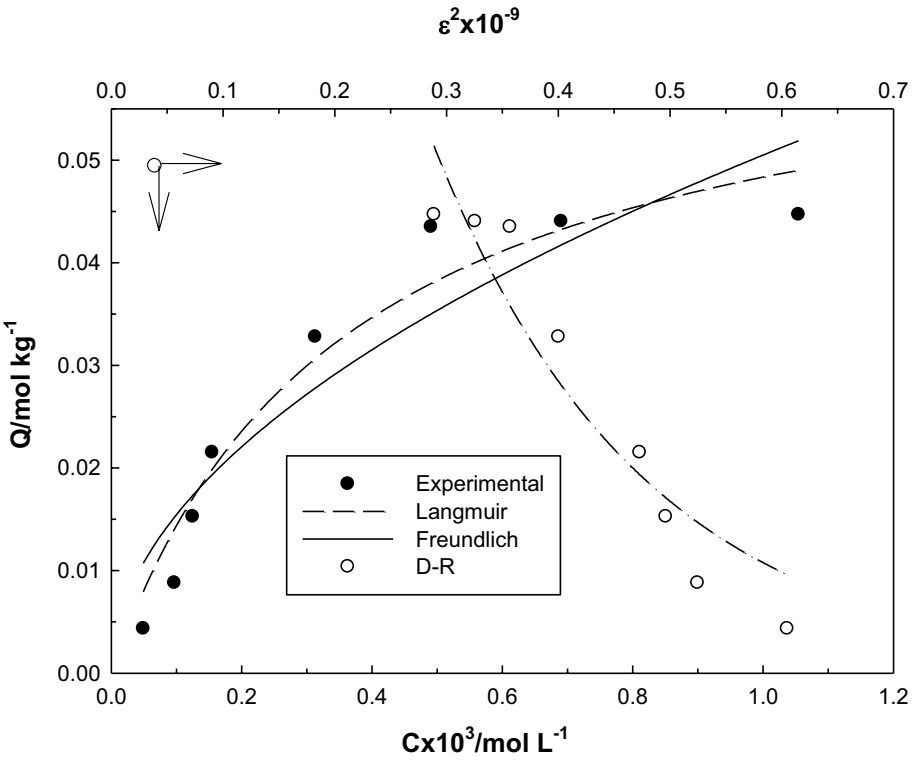

Fig. 7 Experimentally obtained adsorption isotherms UO_2^{2+} onto PAA-K and their compatibility to Langmuir, Freundlich and D-R models {$[UO_2^{2+}]_0$:50–1000 mg L^{-1}, adsorbent dosage:100 mg, natural pH:4.5, contact time:24 h, temperature: 25 °C}

better. The Langmuir isotherm model is an isotherm model [26] describing the adsorption on monolayer and homogeneous surfaces involving the formation of ion exchange and chemical bonding. Single-layer adsorption capacity from the Langmuir isotherm model was found to be 0.0656 mol kg^{-1}. The Langmuir constant was found to be 184 L mol^{-1}. Freundlich isotherm model is the isotherm model [27] that explains the adsorption on multilayer and heterogeneous surfaces related to various physical interactions such as electrostatic interactions and Van der Waals interactions. Freundlich adsorption capacity from Freundlich isotherm model was found to be X_F, 1.76 and surface heterogeneity as 0.154.

The D-R isotherm model is a model used for adsorption on both homogeneous and heterogeneous surfaces and mainly explains the adsorption of pores. Examines the adsorption in terms of energetic [28]. The adsorption energy for UO_2^{2+} ions adsorption to the PAA-K composite was found to be 9.71 kJ mol^{-1}. This indicates that the adsorption process is chemical.

Adsorption kinetics

Adsorption kinetics are required to determine the equilibrium interaction time of adsorption and to determine the optimum conditions in the adsorption process. The speed control steps in the adsorption process, the mass transfer or chemical reaction process, can be found by fitting experimental data into kinetic models. For this purpose, three common kinetic models; Pseudo first order (PFO) [29], pseudo second order (PSO) [30] and intra particle diffusion (IPD) [31] models are used. Equations of these kinetic models are presented in Table 2. Under the conditions of C_0: 400 mg L^{-1}, m: 100 mg, pH: 4.5 and T: 25 °C, the effect of different contact time (10–1440 min) on the adsorption performance of UO_2^{2+} ions were investigated. Compliance with the adsorption kinetic models for UO_2^{2+} ions adsorption to the PAA-K composite is presented in Fig. 8 and the derived kinetic parameters are presented in Table 2. When Fig. 8 was examined, it was seen that the adsorption of UO_2^{2+} ions stabilized within 200 min (5 h). When the correlation coefficients (R^2) of the PFO and PSO models were compared, it was observed that the experimental results fit better with the PSO kinetic model. At the same time, when the experimentally calculated Q_t and theoretically calculated Q_e values were examined, it was found that the results fit the PSO model better. It plays an important role in intra-particle diffusion in the adsorption process. IPD has two linear components that do not pass through the origin. This means that the adsorption process takes place first in the active centers on the PAA-K composite surface and then gradually in the pores of the PAA-K composite. In the light of the kinetic results obtained, the adsorption of UO_2^{2+} ions to the PAA-K composite is explained with PSO and IPD models. First, rapid adsorption takes place, then relatively slow

Table 2 PFO, PSO and IPD kinetic models and their parameters

Kinetic models	Equation	Parameters
PFO	$Q_t = Q_e\left[1 - e^{-k_1 t}\right]$ $H_1 = k_1 Q_e$	Q_t: the adsorbed amount at time Q_e: the adsorbed amount at equilibrium t: time k_1: the rate constant of the PFO H_1: initial adsorption rate for PFO
Parameter	Value	R^2
Q_t/mol kg^{-1}	0.0473	0.502
Q_e/mol kg^{-1}	0.0394	
$k_1 \times 10^3$/min^{-1}	44.7	
$H_1 \times 10^3$/mol kg^{-1} min^{-1}	1.76	
PSO	$Q_t = \frac{t}{\left[\frac{1}{k_2 Q_e^2}\right] + \left[\frac{t}{Q_e}\right]}$	k_2: the rate constant of the PSO model
	$H_2 = k_2 Q_e^2$	H_2: initial adsorption rate for PSO
Parameter	Value	R^2
Q_t/mol kg^{-1}	0.0473	0.706
Q_e/mol kg^{-1}	0.0430	
$k_2 \times 10^3$/mol^{-1} kg min^{-1}	12.7	
$H_2 \times 10^3$/mol kg^{-1} min^{-1}	23.4	
IPD	$Q_t = k_i t^{0.5}$	k_i: the rate constant of the IPD
Parameter	Value	R^2
$k_i \times 10^3$/molkg^{-1} $min^{-0.5}$	15.7	0.971

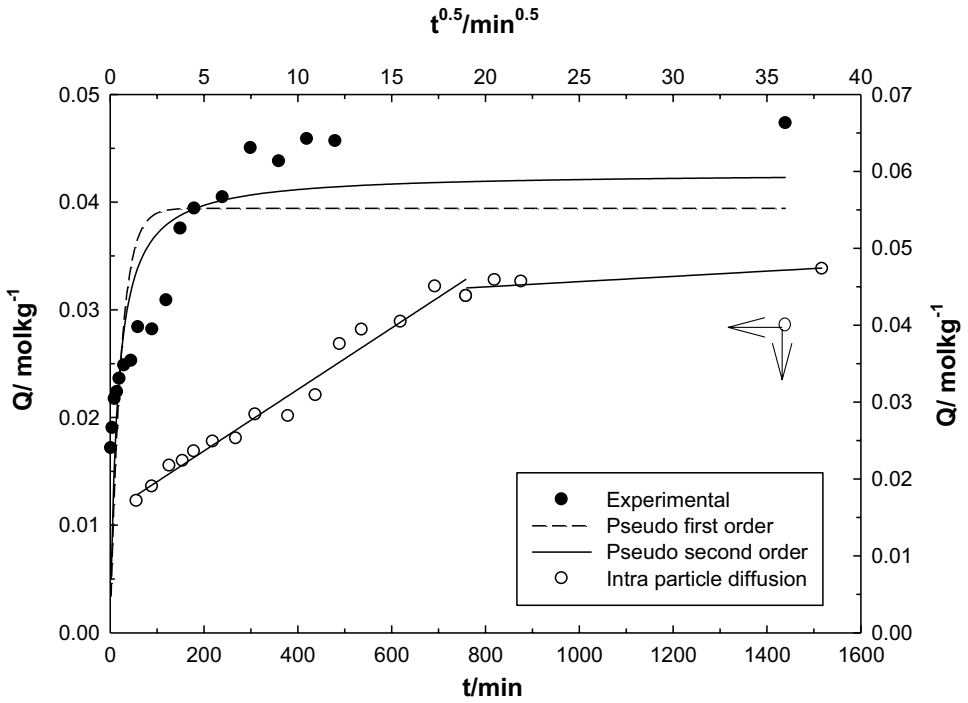

Fig. 8 Compatibility of UO_2^{2+} adsorption kinetics to PFO, PSO and IPD {$[UO_2^{2+}]_0$:400 mg L^{-1}, adsorbent dosage:300 mg, natural pH:4.5, contact time:2–1440 min, temperature:25 °C}

intra-particle diffusion occurs. According to these results, chemical adsorption is dominant in the adsorption process of UO_2^{2+} ions to the PAA-K composite.

Adsorption thermodynamics

Under the conditions of C_0: 400 mg L^{-1}, m: 100 mg, pH: 4.5 and t: 1440 min, the effects of different temperatures (5 °C, 15 °C, 25 °C, 40 °C and 50 °C) on the adsorption of

uranyl ions were investigated. Thermodynamic parameters including enthalpy change (ΔH^0), entropy change (ΔS^0) and free energy change (ΔG^0) were determined [32, 33] using the following equations; The distribution coefficients (K_D) were derived from Eq. (4);

$$K_D = \frac{Q}{C_e} \tag{4}$$

The free energy of adsorption (ΔG^0) is related to K. Thus, Eq. (5) may be written as;

$$\Delta G = -RTlnK_D \tag{5}$$

The value of enthalpy changes (ΔH^0) and entropy changes (ΔS^0) for adsorption was calculated using Eq. (6) in below;

$$\ln K_D = \frac{\Delta S^0}{R} - \frac{\Delta H^0}{RT} \tag{6}$$

Thermodynamic parameters (ΔH^0 and ΔS^0) are obtained from Fig. 9. The slope ($-\Delta H^0/R$) and y-intercept ($\Delta S^0/R$) of the data plotted as $\ln K_D$ against 1/T. Gibbs free energy change was calculated using Eq. (7).

$$\Delta G^0 = \Delta H^0 - T\Delta S^0 \tag{7}$$

Thermodynamic parameters (ΔH^0 and ΔS^0) are obtained from Fig. (9). The slope ($-\Delta H^0/R$) and y-intercept ($\Delta S^0/R$) of the data plotted as $\ln K_D$ against 1/T. ΔH^0 was found as 24.4 kJ mol^{-1}. A positive ΔH^0 value showed that the adsorption process was endothermic. ΔS^0 was calculated as 110 J mol-1 K^{-1}. The positive ΔS^0 value indicated an increase in randomness at the solid–liquid interface during the adsorption process. ΔG^0 was found as -6.22 kJ mol^{-1}, -7.31 kJ mol^{-1}, -8.42 kJ mol^{-1}, -10.1 kJ mol^{-1} and -11.7 kJ mol^{-1} at 5 °C, 15 °C, 25 °C, 40 °C and 50 °C respectively. The thermodynamic parameters $\Delta H > 0$, $\Delta S > 0$ and $\Delta G < 0$, indicated that the adsorption behavior is a endothermic, entropy-increasing and spontaneous at higher temperatures. The thermodynamic data obtained showed that the adsorption process of UO_2^{2+} ions to the PAA-K composite was endothermic, entropy-increasing and spontaneous.

Adsorption–desorption performance

Desorption studies were performed to prove whether the adsorbent used was recyclable. The recovery experiments were repeated five times with the same adsorbent after the adsorption–desorption cycle. To evaluate the recovery/desorption conditions of the adsorbed UO_2^{2+} ions, a series of desorption experiments were performed using HCl, NaOH, HNO_3, and ethanol, and the maximum recovery percentage was obtained with HCl (Fig. 10). After the five adsorption–desorption cycles, the PAA-K composite beads still maintain about 51% of its initial activity. These results may confirm the green and cost-effective value of the synthesized materials for removal and recovery of the UO_2^{2+} ions from aqueous solutions.

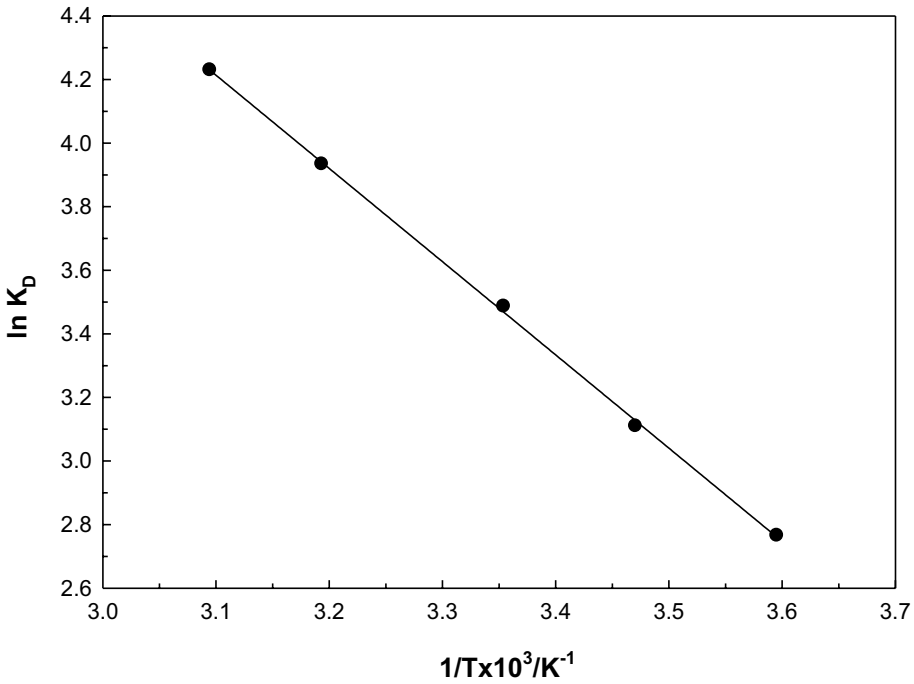

Fig. 9 The effect of temperature on the adsorption. {$[UO_2^{2+}]_0$:400 mg L^{-1}, adsorbent dosage:100 mg, natural pH:4.5, contact time:24 h, temperature: 5 °C, 15 °C, 25 °C, 40 °C and 50 °C}

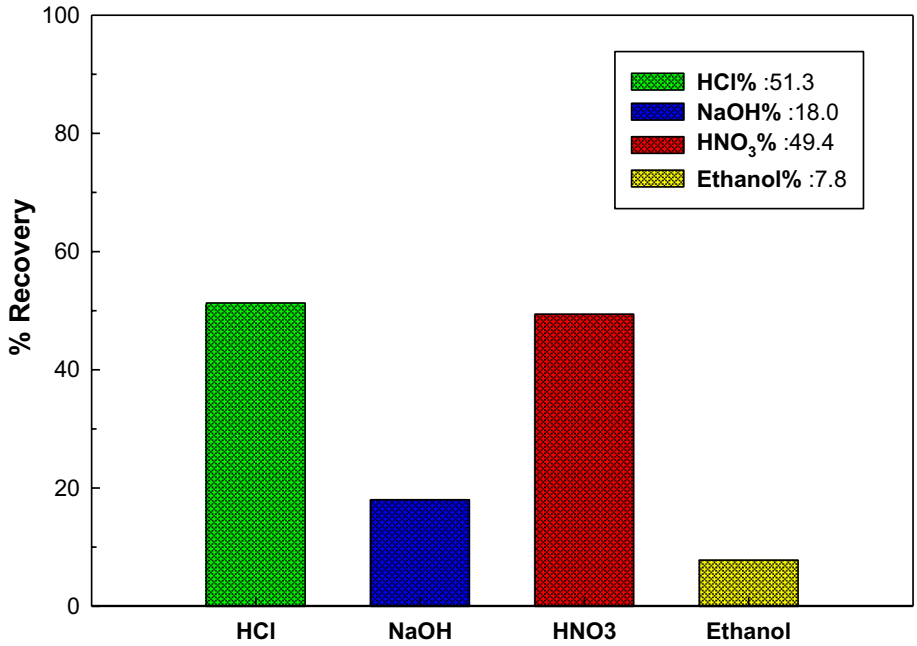

Fig. 10 The effect of recovery for PAA-K. {$[UO_2^{2+}]_0$: 400 mg L^{-1}, adsorbent dosage:100 mg, natural pH:4.5, contact time:24 h, temperature: 25 °C}

Conclusion

PAA-K composite adsorbent was synthesized using kaolinite and polyacrylamide, in-situ polymerization method as synthesis method. The adsorption performance for UO_2^{2+} ions of PAA-K composite was explored. Under the conditions that the initial mass concentration of UO_2^{2+} ions was 400 mg L^{-1}, adsorbent mass was 100 mg, pH: 4.5, contact time was 1440 min and the temperature was 25 °C, the maximum adsorption capacity of the PAA-K composite for UO_2^{2+} ions is 0.0656 mol kg^{-1} from the Langmuir isotherm model. The adsorption energy found to be 9.71 kJ mol^{-1}, calculated from the D-R isotherm model, indicated that the nature of the adsorption process was chemical. The kinetic results indicated that the adsorption process followed the PSO and IPD kinetics. The thermodynamic parameters indicated that the adsorption process was an endothermic and spontaneous process. Desorption studies revealed that the PAA-K composite could be recyclable. All obtained results showed that it was manifest that we have successfully prepared the PAA-K composite adsorbent and the PAA-K composite had very good properties such as high adsorption capacity for UO_2^{2+} ions, high adsorption rate, and thermodynamically favorable, easy and economic preparation, environmental friendly, effective and cheap adsorbent.

Acknowledgements The present study was partly supported by Sivas Cumhuriyet University Scientific Research Projects Commission.

References

1. Jiang M, Jin X, Lu XQ, Chen Z (2010) Adsorption of Pb(II), Cd(II), Ni(II) and Cu(II) onto natural kaolinite clay. Desalination 252:33–39
2. Dim PE, Mustapha LS, Termtanun M, Okafor JO (2021) Adsorption of chromium (VI) and iron (III) ions onto acid-modified kaolinite: Isotherm, kinetics and thermodynamics studies. Arab J Chem 14:103064
3. Yangyang Gao WT, Yuan Y, Ma D, Li L, Li Y, Xu W (2014) Removal of aqueous uranyl ions by magnetic functionalized carboxymethylcellulose and adsorption property investigation. J Nucl Mater 453:82–90
4. Zahakifar F, Charkhi A, Torab-Mostaedi M, Davarkhah R, Yadollahi A (2018) Effect of surfactants on the performance of hollow fiber renewal liquid membrane (HFRLM): a case study of uranium transfer. J Radioanal Nucl Chem 318:973–983
5. Mellah A, Chegrouche S, Barkat M (2007) The precipitation of ammonium uranyl carbonate (AUC): thermodynamic and kinetic investigations. Hydrometallurgy 85:163–171
6. Khanramaki F, Shirani AS, Safdari J, Torkaman R (2018) Investigation of liquid extraction and thermodynamic studies on uranium from sulfate solution by Alamine 336 as an extractant. Int J Env Sci Technol 15:1467–1476
7. Yanxia Cheng SW, He P, Dong F, Nie X, Ding C, Ying Zhang SZ, Liu H (2019) Polyamine and amidoxime groups modified bifunctional polyacrylonitrilebased ion exchange fibers for highly efficient extraction of U(VI) from real uranium mine water. Chem Eng J 367:198–207
8. Christou C, Philippou K, Krasia-Christoforou T, Pashalidis I (2019) Uranium adsorption by polyvinylpyrrolidone/chitosan blended nanofibers. Carbohydr Polym 219:298–305
9. Chang-fu W, Zhi-rong L, Gui-rong X, Yi L, Yun W, Li-min Z (2016) Adsorptive properties of sunflower seed shells for UO22+ in aqueous solution. J Nuc Radiochem 38:107–115

10. Sureshkumar MK, Das D, Mallia MB, Gupta PC (2010) Adsorption of uranium from aqueous solution using chitosan-tripolyphosphate (CTPP) beads. J Hazard Mater 184:65–72
11. Şenol ZM, Şimşek S, Özer A, Şenol Arslan D (2021) Synthesis and characterization of chitosan–vermiculite composite beads for removal of uranyl ions: isotherm, kinetics and thermodynamics studies. J Radioanal Nucl Chem 327:159–173
12. Camacho LM, Deng S, Parra RR (2010) Uranium removal from groundwater by natural clinoptilolite zeolite: Effects of pH and initial feed concentration. J Hazard Mater 175:393–398
13. Zahran F, El-Maghrabi HH, Hussein G, Abdelmaged SM (2019) Fabrication of bentonite based nanocomposite as a novel low cost adsorbent for uranium ion removal. Env Nanotechnol Monit Manag 11:100205
14. Cheira MF, Kouraim MN, Zidan IH, Mohamed WS, Hassanein TF (2020) Adsorption of U(VI) from sulfate solution using montmorillonite/polyamide and nano-titanium oxide/polyamide nanocomposites. J Env Chem Eng 8:104427
15. Şenol ZM, Şimşek S, Ulusoy Hİ, Özer A (2020) Synthesis and characterization of a polyacrylamide-dolomite based new composite material for efficient removal of uranyl ions. J Radioanal Nucl Chem 324:317–330
16. Gül ÜD, Şenol ZM, Gürsoy N, Şimşek S (2019) Effective UO22+ removal from aqueous solutions using lichen biomass as a natural and low-cost biosorbent. J Env Radioact 205–206:93–100
17. Hou J, Wang H, Zhang H (2020) Zirconium metal-organic framework materials for efficient ion adsorption and sieving. Ind Eng Chem Res 59:12907–12923
18. Omara SS, Turky G, Ghoneim A, Thünemann AF, Abdel Rehim MH, Schönhals A (2017) Hyperbranched poly(amidoamine)/kaolinite nanocomposites: structure and charge carrier dynamics. Polymer (Guildf) 121:64–74
19. Deng L, Shi Z (2015) Synthesis and characterization of a novel Mg-Al hydrotalcite-loaded kaolin clay and its adsorption properties for phosphate in aqueous solution. J Alloy Compd 637:188–196
20. Şenol ZM (2021) A chitosan-based composite for adsorption of uranyl ions; mechanism, isothems, kinetics and thermodynamics. Int J Biol Macromol 183:1640–1648
21. Cheng H, Liu Q, Yang J, Ma S, Frost RL (2012) The thermal behavior of kaolinite intercalation complexes-A review. Thermochim Acta 545:1–13
22. Belver C, Bañares Muñoz MA, Vicente MA (2002) Chemical activation of a kaolinite under acid and alkaline conditions. Chem Mater 14:2033–2043
23. Sari A, Tuzen M, Soylak M (2007) Adsorption of Pb(II) and Cr(III) from aqueous solution on Celtek clay. J Hazard Mater 144:41–46
24. Shaikh SH, Kumar SA (2017) Polyhydroxamic acid functionalized sorbent for effective removal of chromium from ground water and chromic acid cleaning bath. Chem Eng J 326:318–328
25. Ilaiyaraja P, Singha Deb AK, Sivasubramanian K, Ponraju D, Venkatraman B (2013) Adsorption of uranium from aqueous solution by PAMAM dendron functionalized styrene divinylbenzene. J Hazard Mater 250–251:155–166
26. Langmuir I (1981) The adsorption of gases on plane surfaces of glass mica and platinum. J Am Chem Soc 40:1361–1403
27. Freundlich HMF (1906) Over the adsorption in solution. Zeitschrift für Phys Chemie 57:385–471
28. Dubinin MM, Zaverina ED (1947) Sorption and structure of active carbons. I. adsorption of organic vapors. Zhurnal Fiz Khimii 21:1351–1362
29. Ho G, McKay YS (1999) Pseudo-second-order model for sorption processes. Process Biochem 34:451–465
30. Crini G, Badot PM (2008) Application of chitosan, a natural aminopolysaccharide, for dye removal from aqueous solutions by adsorption processes using batch studies: A review of recent literature. Prog Polym Sci 33:99–447
31. Varma AJ, Deshpande SV, Kennedy JF (2004) Metal complexation by chitosan and its derivatives: a review. Carbohydr Polym 55:77–93
32. Ammendola P, Raganati F, Chirone R (2017) CO_2 adsorption on a fine activated carbon in a sound assisted fluidized bed: Thermodynamics and kinetics. Chem Eng J 322:302–313
33. Mijinyawa AH, Durga G, Mishra A (2019) A sustainable process for adsorptive removal of methylene blue onto a food grade mucilage: kinetics, thermodynamics, and equilibrium evaluation. Int J Phytoremediation 21:1122–1129